

Isotopic Mo Neutron Total Cross Section Measurements in the Energy Range 1 to 620 keV

R. Bahran,^{1,*} D. Barry,² G. Leinweber,² M. Rapp,² R. Block,²
A. Daskalakis,¹ B. McDermott,¹ S. Piela,¹ E. Blain,¹ and Y. Danon¹

¹Gaerttner LINAC Center, Rensselaer Polytechnic Institute, Troy, NY 12180, USA

²Bechtel Corp., Knolls Atomic Power Laboratory, P.O. Box 1072, Schenectady, NY 12301, USA

A series of new total cross section measurements for the stable molybdenum isotopes of ^{92,94,95,96,98,100}Mo covering the energy range between 1 keV and 620 keV was performed at the Gaerttner LINAC Center at Rensselaer Polytechnic Institute. New high-accuracy resonance parameters were extracted from an analysis of the data using the multilevel R-matrix Bayesian code SAMMY. In the unresolved resonance region, average resonance parameters and fits to the total cross sections were obtained using the Bayesian Hauser-Feshbach statistical model code FITACS.

I. INTRODUCTION

The Gaerttner LINAC Center at Rensselaer Polytechnic Institute is home to a 60 MeV electron linear accelerator (LINAC) that is used as a pulsed neutron source for time-of-flight nuclear data measurements. High energy resolution total cross section measurements were performed with the Mid-Energy ⁶Li-glass Neutron Detector Array (MELINDA) [1] positioned at 100 meters. The measurements provide transmission data that cover the energy range between 1 keV and 620 keV for the stable molybdenum isotopes of ^{92,94,95,96,98,100}Mo. Accurate isotopic molybdenum total cross section data are of particular importance because stable Mo isotopes can be found in significant concentrations in a nuclear fuel cycle either as a high yield fission product or in alloyed form with applications in reactor piping, fuel cladding, and most importantly as an advanced nuclear fuel in the form of U-Mo [2, 3]. The measured energy range encompasses the resolved resonance region and extends into the unresolved resonance region for each isotope. In the resolved resonance region, new high-accuracy resonance parameters were extracted from fitting experimental data using the multilevel R-matrix Bayesian code SAMMY [4]. In the unresolved resonance region, average resonance parameters and fits to the total cross sections were obtained using the Bayesian Hauser-Feshbach statistical model code FITACS [5] which is embedded in SAMMY.

II. MEASUREMENTS

Transmission measurements were performed with the Mid-Energy ⁶Li-glass Neutron Detector Array (MELINDA) which is stationed 100 meters away from a water-moderated tantalum photoneutron target [6]. The detector employs four identical cube-shaped modules consisting of a 0.5-inch thick ⁶Li-glass scintillator, two out-of-neutron-beam photomultiplier tubes, and a low-mass, light-tight aluminum casing with inner reflective surfaces. Fast-timing modular electronics were employed to take full advantage of the fast ⁶Li-glass scintillator response time and the short neutron burst width. More information on the detector can be found in Reference [1].

Highly-enriched metallic isotopic molybdenum samples were prepared by Oak Ridge National Laboratory. More information on the characteristics of the measured samples can be found in Ref. [11]. The samples were stacked and mounted to a computer-controlled sample changer located at a distance ≈ 13 m from the photoneutron target. Transmission measurements were performed by placing each molybdenum sample in a collimated neutron beam and measuring the number of neutrons passing through the sample and subsequently interacting with the detector. This value is then compared with the number of neutrons detected when there is no sample in the beam. The measurements utilized a fixed ¹⁰B-enriched boron disc (0.0448 atoms/barn) to minimize overlap neutrons between neutron pulses. Additionally, a high-Z filter was inserted in the beam (0.5-inch Pb or 1-inch ²³⁸U) to reduce the low-energy γ -ray background and the initial high-energy bremsstrahlung radiation burst generated by the target. A new method to characterize and quantify the different background components (neutron and γ -ray)

* Corresponding author: bahrar@rpi.edu

was performed by cycling different filter materials into the beam line. Three major background components were observed in the transmission experiments. The smallest component was the constant time-independent environmental “room” background. The dominant time-dependent γ -ray background component was determined by placing several thicknesses of polyethylene in the beam and extrapolating to zero-thickness polyethylene. An experiment utilizing D₂O in place of H₂O as the target moderator showed that the γ -ray background was mainly a result of thermal neutron capture in hydrogen. Finally, strong resonances in Na, Al, Mg, S, Li, and Be were used to determine the time-dependent neutron background component at 2.8 keV, 35 keV, 83 keV, 103 keV, 250 keV, and 620 keV respectively. The observed count rate for the open beam and all three background components are shown in Fig. 1.

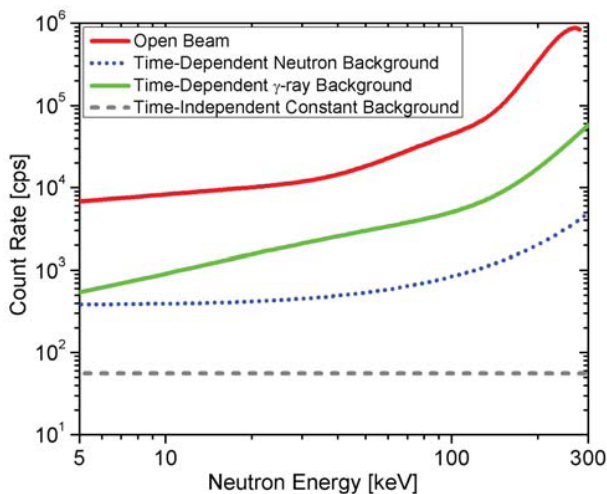


FIG. 1. Decomposition of the background shapes observed by the ⁶Li-glass modular detector.

The new high-resolution data include newly-resolved resonances that can be used to extend the resolved resonance region for each molybdenum isotope. In the resolved resonance region, the R-matrix code SAMMY was used to obtain resonance parameters. Several important input parameters were required for data analysis using SAMMY in the resolved resonance region. These parameters included information on the target nucleus, experimental conditions (summarized in Table I), and a good first-order approximation of a starting set of resonance parameters. The flight path was fitted to ²³⁸U transmission data. The uncertainty in the flight path (Δl) was estimated as the thickness of the scintillator combined with a neutron mean free path in the moderator in the energy range of interest (20 - 50 keV for the value in Table I).

The energy-dependent resolution function was found to have a functional form represented by the convolution of a Gaussian and an exponential. The width of the Gaussian represents the distribution in time (or energy) of neutrons

TABLE I. SAMMY experimental input conditions.

Input Parameter	Value
Flight Path Length	100.125 m
Δ Flight Path Length (FWHM)	0.025 m
Electron Burst Width (FWHM)	0.011 μ s
Channel Width (Rectangular)	0.0064 μ s
Sample Temperature	293 K

as contributed by the moderator, scintillator, burst width and time-of-flight clock channel width. These widths in energy are shown in Fig. 2. The contribution from the detector scintillator and target moderator (Δl) is dominant at lower energies. In the unresolved region, the burst width dominates. The exponential component represents the energy distribution asymmetry as contributed from both the moderator and scintillator. This exponential “tail” was also present in Monte Carlo simulations of the target and detector. The magnitude of the tail was fitted along with the resonance parameters at several narrow p-wave resonances in the isotopic molybdenum data over the energy range of interest.

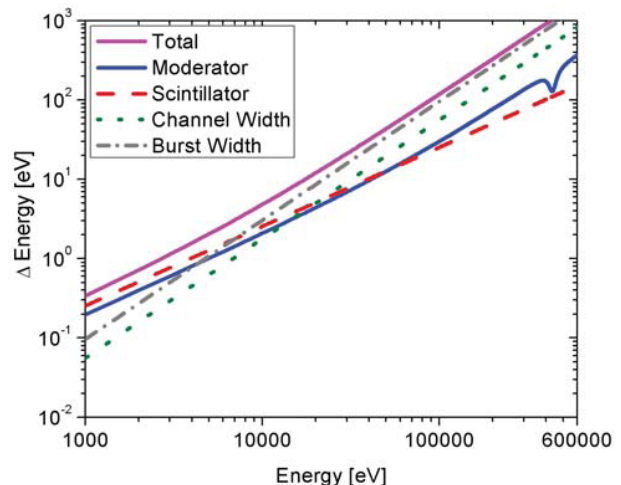


FIG. 2. Gaussian width of the experimental resolution for different components.

Two general guides to fitting individual resonances in the resolved resonance region were followed [7, 8]. Individual resonance neutron widths and energies were allowed to vary. Radiative widths for s-waves were only varied if their ratio to the neutron width was less than 5, in accordance with the radiation width sensitivity factor previously implemented by Barry [8, 9]. Different spins for each fitted resonance were assigned based on a χ^2 goodness of fit test. A snippet of the experimental isotopic Mo total cross section data with example fits to several new resonances is shown in Fig. 3. In this region, ENDF/B-VII.1 represents the total cross section as a smooth unresolved average cross section.

At some point in energy, only partially resolved struc-

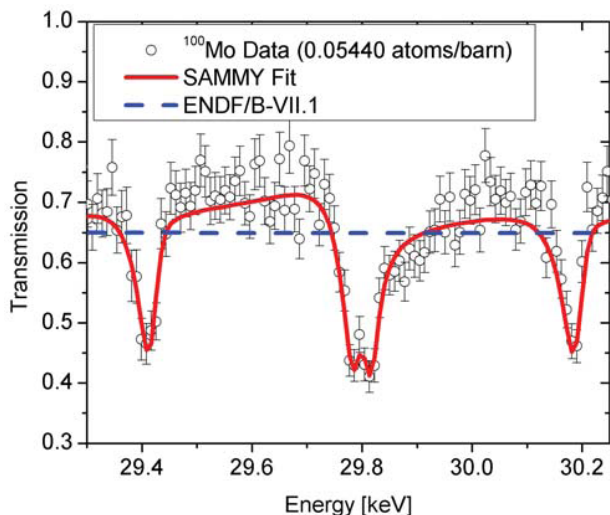


FIG. 3. SAMMY fits to newly observed resonances in ^{100}Mo .

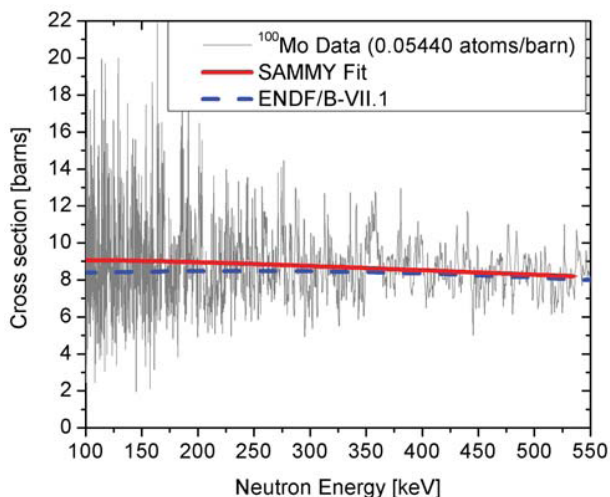


FIG. 4. SAMMY ^{100}Mo average total cross section fit in the unresolved resonance region.

ture is observed and a transition into the unresolved

resonance region occurs. Evaluation in this region was performed with the Bayesian Hauser-Feshbach statistical model code FITACS, which is currently incorporated into the SAMMY Bayesian analysis code. A SAMMY fit to the ^{100}Mo total cross section in the unresolved region is shown in Fig. 4. Average resonance parameters and covariance matrices were obtained from SAMMY fits in this region in a format compatible with ENDF.

III. CONCLUSIONS

A series of new total cross section measurements for the stable molybdenum isotopes of $^{92,94,95,96,98,100}\text{Mo}$ provided resonance parameter sets in the energy range between 1 keV and 620 keV spanning both the resolved and unresolved resonance region. The measured data is in good agreement with the current resolved region in ENDF/B-VII.1 which extends up to 2.2 keV for ^{95}Mo , 19 keV for ^{96}Mo , 26 keV for ^{100}Mo , and 30 keV for ^{98}Mo . The characterization of new resonances extended the resolved range for each isotope, especially in ^{95}Mo where it provides the largest contribution to nuclear data libraries. New fits to the total cross section in the unresolved resonance region (URR) were also obtained. Overall, the maximum deviations from the current ENDF/B-VII.1 evaluation in the URR is up to 10%. Additionally, average resonance parameters were obtained in the unresolved region, providing a new distribution for “ladders” of sampled resonances. These ladders (based on both average parameters and statistical laws) can be used to generate probability tables for Monte Carlo codes in order to represent structure in the unresolved region [10].

Acknowledgements: The authors would like to thank Peter Brand, Matt Gray, Martin Strock and Azzedine Kerdoun for their efforts in operating the LINAC and their help in setting up experiments. They would also like to thank Luiz Leal, Tom Sutton, Paul Romano, Cecil Lubitz and Tim Trumbull for helpful discussion regarding theory and analysis in the unresolved resonance region.

-
- [1] R. Bahran *et al.*, Proceedings of Tenth International Topical Meeting on Nuclear Applications of Accelerators, AccApp’11, Knoxville, TN, 174 (2011).
 - [2] L. Mason *et al.*, Proceedings of Nuclear and Emerging Technologies for Space in Albuquerque, NM **3318** (2011).
 - [3] J. Rest *et al.*, ARGONNE NATIONAL LABORATORY ANL-09/31 (2009).
 - [4] N. Larson, OAK RIDGE NATIONAL LABORATORY, ORNL/TM-9179/R8 (2008).
 - [5] F. Frohner, NUCL. SCI. ENG. **103**, 119 (1989).
 - [6] M. Overberg *et al.*, NUCL. INSTRUM. METHODS PHYS. RES. A **438**, 253 (1999).
 - [7] L.C. Leal *et al.*, Proceedings of the Workshop on Nuclear Reaction Data and Nuclear Reactors: Physics, Design and Safety, Trieste, Italy **Volume I** (2000).
 - [8] D. Barry, PhD Thesis, Rensselaer Polytechnic Institute (2003).
 - [9] G. Leinweber *et al.*, NUCL. SCI. ENG. **164**, 287 (2010).
 - [10] L. Levitt, NUCL. SCI. ENG. **49**, 450 (1972).
 - [11] R. Bahran, PhD Thesis, Rensselaer Polytechnic Institute (2013).